NOVEL OPTICALLY RESPONSIVE AND DIFFRACTING MATERIALS DERIVED FROM CRYSTALLINE COLLOIDAL ARRAY SELF ASSEMBLY

S. A. Asher, J. Weissman, H. B. Sunkara[1], G. Pan, J. Holtz, Lei Liu, and R. Kesavamoorthy[2]

Department of Chemistry, University of Pittsburgh, Pittsburgh, PA 15260
[1]Current address: Space Science Laboratory, NASA, George C. Marshall Space Flight Center, Marshall Space Flight Center, AL 35812
[2]Permanent address: Materials Science Division, Indira Gandhi Centre for Atomic Research, Kalpakkam 603102 Tamilnadu, India

Novel tunable and switchable diffracting devices useful in the UV, visible and IR region are fabricated through self assembly of monodisperse, highly charged colloidal particles into crystalline colloidal arrays (CCA). The particles form BCC or FCC arrays with spacings that diffract light. We fabricated devices where the particle size or spacing changes with temperature to tune the diffraction. We also fabricated nonlinear devices which switch in ~3 ns. This CCA utilizes dyed particles, which are index matched to the medium. No light is diffracted at low intensities, but at high intensities the particles heat up, their index mismatches from the medium to turn the CCA diffraction on within 5 ns.

Crystalline colloidal arrays (CCA) are mesoscopically periodic fluid materials which efficiently diffract light meeting the Bragg condition (*1-4*). These materials consist of arrays of colloidal particles which self assemble in solution into BCC or FCC crystalline arrays (*1,5*) (Figure 1) with lattice constants in the mesoscale size range (50 to 500 nm). Just as atomic crystals diffract x-rays that meet the Bragg condition, CCA diffract UV, visible, and near IR light (*2-4*); the diffraction phenomena resemble that of opals, which are close-packed arrays of monodisperse silica spheres (*6*).

The CCA, however, can be prepared as macroscopically ordered arrays of non-close-packed spheres. This self assembly is the result of electrostatic repulsions between colloidal particles, each of which has numerous charged surface functional groups. We have concentrated on the development of CCA which diffract light in the visible spectral region, and have generally utilized colloidal particles of ca. 100 nm diameter (*7*). These particles have thousands of charges which result from the ionization of sulfonate groups attached to the particle surfaces. The nearest neighbor distances are often ca. 200 nm.

Optical Diffraction Devices

These BCC or FCC cubic arrays are well ordered and the arrays strongly diffract light in the visible spectral region (Figure 2). All light meeting the Bragg condition is diffracted while adjacent spectral regions freely transmit. We earlier demonstrated the use of these devices as narrow-band optical diffraction filters (*1c,3,8,9*). We more recently developed methods (*10-12*) to solidify and rigidize these arrays by imbedding the CCA cubic lattice in a hydrogel polyacrylamide matrix (Figure 3). This system can be prepared such that the acrylamide and the colloidal particles occupy a small percent of the sample volume, which mostly consists of water. The medium surrounding the spheres can be modified since other solvents can be diffused into the polymerized array to replace the water. Although the hydrogel-linked CCA undergoes swelling and shrinkage as the solvent medium is changed, the array ordering is maintained. Films of this array can be prepared where the (110) plane of the BCC lattice is well oriented and parallel to the surface. The (110) planes of the periodic colloidal structure in the film strongly diffract light meeting the Bragg condition.

Thermally Tunable Diffraction Devices

More recently we utilized the well-known temperature-induced volume phase transition properties of poly(N-isopropylacrylamide) (PNIPAM) (*13-15*) to create novel CCA materials with variable sphere size and variable array periodicity (*16*). In water below ~30°C, PNIPAM is hydrated and swollen, but when heated above its lower critical solution temperature (~32°C) it undergoes a reversible volume phase transition to a collapsed, dehydrated state. The temperature increase causes the polymer to expel water and shrink into a more hydrophobic polymer state.

We developed a synthesis of monodisperse, highly charged colloidal particles of PNIPAM whose diameter depends on temperature (*16*). NIPAM was polymerized with the ionic comonomer 2-acrylamido-2-methyl-1-propane sulfonic acid to increase the colloid surface charge which facilitates CCA self-assembly. Figure 4 shows the temperature dependence of the colloidal sphere diameter, which increases from ~100 nm at 40°C to ~300 nm at 10°C.

These PNIPAM colloids self-assemble in deionized water to form CCA both above and below the polymer phase transition temperature. The ordered array diffracts light almost following Bragg's diffraction law (but not exactly as shown elsewhere (*4*)):

$$m\lambda = 2nd\sin\theta \qquad (1)$$

where m is the order of diffraction, λ is the wavelength of incident light, n is the suspension refractive index, d is the interplanar spacing, and θ is the glancing angle between the incident light and the diffracting crystal planes (*4*), which are oriented parallel to the crystal surface in the CCA we prepare. Figure 5 shows the resulting extinction spectra of a PNIPAM CCA at 10°C and 40°C. At low temperatures, the CCA particles are highly swollen, almost touching, and diffract weakly. Above the

phase transition temperature, these particles become compact, increase their refractive index and diffract nearly all incident light at the Bragg wavelength. The temperature change does not affect the lattice spacing. This material acts as a thermally controlled optical switch.

In addition, we used a similar concept (*16*) to fabricate wavelength-tunable diffraction devices using a PNIPAM gel to control the periodicity of the CCA. We polymerized a CCA of polystyrene (PS) spheres in PNIPAM. This polymerized CCA film (PCCA) shrinks and swells continuously and reversibly between 10°C and 35°C; the embedded PS sphere array follows, changing the lattice spacing and thus the diffracted wavelength (Figure 6). The inset to Figure 6 shows the temperature dependence of the diffracted wavelength for this PCCA film, where the incident light is normal to the (110) plane of the lattice.

This PCCA film functions as a tunable optical filter; the diffracted wavelength can be altered by varying either the temperature or the angle of incidence. At a fixed angle to the incident beam this PCCA acts as a tunable wavelength reflector. The width and height of the diffraction peak can be easily controlled by choosing colloidal particles of different sizes and refractive indices or by making different thickness PCCA films (*16*). The tuning range of this device can be widened or narrowed by synthesizing PCCA films with lower or higher cross-linking concentrations.

Improved Diffraction Efficiencies

We also prepared CCA of silica colloidal spheres of ~100-nm diameter and examined their diffraction characteristics over a wide wavelength range. Figure 7 shows the extinction peaks for the primary and secondary diffraction from this CCA for normal incidence. The primary diffraction at 606 nm results from first order diffraction from the (110) BCC planes, while the 315 nm secondary diffraction results from the combination of first order diffraction from numerous higher index planes of the BCC CCA lattice and second order diffraction from the (110) plane. The secondary diffraction efficiency of the BCC CCA is dramatically increased at $\lambda_0/2$ (more than 10-fold) compared to the λ_0 diffraction efficiency (*4*). This anomalous efficiency increase is due to the orientation of numerous higher index planes which fortuitously diffract light at $\lambda_0/2$. This increased diffraction efficiency will increase the response of the nonlinear CCA optical switches described below.

Nonlinear Optical Diffracting Elements

We earlier suggested that we could build nonlinear optical switching materials (*8,17-19*) by creating a CCA of optically nonlinear colloidal particles. One approach would utilize organic polymer spheres containing a dye. We would adjust the composition of the medium such that the real part of the refractive index of the spheres was identical to that of the medium (*18c*). Thus, the array would not diffract light which meets the Bragg condition. At high incident light intensities, however, significant heating would occur within the colloidal particles, the temperature would increase, the refractive index would decrease, and the array

would "pop up" to diffract light. We calculated that the switching time could be within 5 nsec for pulsed laser sources (*18c*).

We synthesized 138-nm diameter monodisperse colloidal particles of heptafluorobutyl methacrylate and covalently attached acylated Oil Blue N dye to these colloidal spheres. These monodisperse highly charged fluorinated colloids have the lowest refractive index (n=1.386) of any monodisperse colloid known. These fluorinated colloids self-assemble into a CCA which was polymerized within an acrylamide hydrogel. Dimethyl-sulfoxide was added to the mainly aqueous medium in order to adjust the medium refractive index to either slightly above or slightly below that of the colloidal particles.

Diffraction by the array was monitored using the experimental apparatus shown in Figure 8. The 532 nm pump beam derived from a Coherent Inc. Infinity frequency doubled YAG laser. The probe beam derived from a dye laser pumped by the 532 nm beam. The pump and the probe beams were ca. 3.5 nsec duration, and were made coincident on the sample, but the probe beam was adjusted temporally such that it was delayed by ca. 2.5 nsec compared to the pump beam. The relative angle of the sample to the probe beam was adjusted such that the Bragg condition was met. If the refractive indices were exactly matched no diffraction should be observed in the absence of the pump beam. If the refractive index of the colloidal particles was adjusted to be slightly greater or less than that of the medium a small fraction of the probe beam will diffract.

Figure 9 shows the extinction spectrum of this dyed crystalline colloidal array hydrogel film measured at normal incidence. The broad 520 nm band results from colloidal particle dye absorption. The 640 nm peak results from the BCC (110) plane Bragg diffraction. The film was oriented such that its normal made an angle of ca. 15° relative to the incident beam, such that light at the dye laser output at 594 nm would be diffracted. Figure 10 shows three measurements where the medium has a refractive index of either 1.3813 or 1.3908, which is either below or above the sphere refractive index, or for a PCCA without dye. Figure 10 plots the relative value of the diffracted light intensity at various pump energy values compared to the value in the absence of the pump laser. As expected, if the colloid refractive index is below that of the medium, incident beam heating further decreases the colloid refractive index below that of the medium and the diffracted intensity increases. In contrast, if the colloid refractive index is above that of the medium, pump beam heating decreases the refractive index towards that of the medium and the diffraction decreases. Without dye no nonlinear response appears. Thus, we have now observed our previously predicted nonlinear optical switching behavior from CCA. We are continuing refinement of the optical materials described here.

Acknowledgments. The authors gratefully acknowledge financial support from the Office of Naval Research through Grant No. N00014-94-1-0592, Air Force Office of Scientific Research through Grant No. F49620-93-1-0008, and from the University of Pittsburgh Materials Research Center through the Air Force Office of Scientific Research Grant No. AFOSR-91-0441.

Literature Cited

(1) The physics of crystalline colloidal array ordering and phase transitions is quite extensive with a few hundred references over the last 30 years. The following recent publications are excellent reviews.
(a) Thirumalai, D. *J. Phys. Chem.* **1989,** *93*, 5637. (b) Walsh, A. M.; Coalson, R. D. *J. Chem. Phys.* **1994,** *100*, 1559. (c) Asher, S. A., U.S. Patents **1986,** #4,627,689, 4,632,517 and **1995,** #5,452,123. (d) Hiltner, P.A.; Krieger, I. M. *J. Phys. Chem.* **1969**, *73*, 2386. (e) Clark, N. A.; Hurd, A. J.; Ackerson, B. J. *Nature* **1979**, *281*, 57. (f) Alexander, S.; Chaikin, P. M.; Grant, P.; Morales, G. J.; Pincus, P.; Hone, D. *J. Chem. Phys.* **1984,** *80*, 5776. (g) Monovoukas, Y; and Gast, A. P. *J. Colloid Interface Sci.* **1989,** *128*, 533. (h) Krieger, I. M.; O'Neill, F. M. *J. Am. Chem. Soc.* **1968,** *90*, 3114. (i) Luck, V. W.; Klein, M.; Wesslau, H.; *Ber. Bunsenges, Physik. Chem.* **1963**, *67*, 75. (j) Hone, D.; Alexander, S.; Chaikin, P. M.; Pincus, P. *J. Chem. Phys.* **1983,** *79*, 1474.

(2) Carlson, R. J.; Asher, S. A. *Appl. Spectrosc.* **1984**, *38*, 297.

(3) (a) Flaugh, P. L.; O'Donnell, S. E.; Asher, S. A. *Appl. Spectrosc.* **1984**, *38*, 847. (b) Asher, S. A.; Flaugh, P. L.; Washinger, G. *Spectrosc.* **1986**, *1*, 26.

(4) Rundquist, P. A.; Photinos, P.; Jagannathan, S.; Asher, S. A *J. Chem. Phys.* **1989**, *91*, 4932.

(5) Zahorchak, J. C.; Kesavamoorthy, R.; Coalson, R. D.; Asher, S. A. *J. Chem. Phys.* **1982**, *96*, 6874.

(6) Sanders, J. V. *Nature* **1964**, *204*, 1151.

(7) (a) Rundquist, P. A.; Jagannathan, S.; Kesavamoorthy, R.; Brnardic, C.; Xu, S.; Asher, S. A. *J. Chem. Phys.* **1981**, *94*, 711. (b) Kesavamoorthy, R.; Jagannathan, S.; Rundquist, P. A.; Asher, S. A. *J. Chem. Phys.* **1991**, *94*, 5172. (c) Rundquist, P. A.; Kesavamooorthy, R.; Jagannathan, S.; Asher, S. A. *J. Chem. Phys.* **1991**, *95*, 1249. (d) Rundquist, P. A.; Kesavamoorthy, R.; Jagannathan, S.; Asher, S. A. *J. Chem. Phys.* **1991**, *95*, 8546.

(8) Spry, R. J.; Kosan, D. J. *Appl. Spectrosc.* **1986**, *40*, 782.

(9) (a) Sunkara, H. B.; Jethmalani, J. M.; Ford, W. T. *Chem. Mater.* **1994**, *6*, 362. (b) Sunkara, H. B.; Jethmalani, J. M.; Ford, W. T. *ACS Symp. Ser.* **1995**, *585*, 181.

(10) Asher, S. A.; Holtz, J.; Liu, L.; Wu, Z. *J. Am. Chem. Soc.* **1994**, *116*, 4997.

(11) Asher, S. A.; Jagannathan, S. U. S. Patent, **1994,** #5 281 370.

(12) Haacke, G.; Panzer, H. P.; Magliocco, L. G.; Asher, S. A. U. S. Patent 5 266 238, **1993**.

(13) Hirokawa, Y.; Tanaka, T. *J. Chem. Phys.* **1984**, *81*, 6379.

(14) Schild, H. G. *Prog. Polym. Sci.* **1992**, *17*, 163.

(15) Wu, X. S.; Hoffman, A. S.; Yager, P. *J. Polym Sci. Part A: Polym. Chem.* **1992**, *30*, 2121.

(16) Weissman, J.; Sunkara, H. B.; Tse, A. S.; Asher, S. A. *Science* **1996**, *274*, 959.

(17) (a) Asher, S. A.; Chang, S.-Y.; Tse, A.; Liu, L; Pan, G.; Wu, Z.; Li, P. *Mat. Res. Soc. Symp. Proc.* **1995**, *374*, 305. (b) Asher, S. A.; Kesavamoorthy, R.; Jagannathan, S.; Rundquist, P. *SPIE Vol. 1626 Nonlinear Optics III*, **1992**, 238. (c) Asher, S. A.; Chang, S.-Y.; Jagannathan, S.; Kesavamoorthy, R.; Pan, G., U. S. Patent, **1995,** #5 452 123.

(18) (a) Chang, S.-Y.; Liu, L.; Asher, S. A. *Mat. Res. Soc. Symp. Proc.* **1994**, *346*, 875. (b) Chang, S.-Y.; Liu, L.; Asher, S. A. *J. Am. Chem. Soc.* **1994**, *116*, 6739. (c) Kesavamoorthy, R.; Super, M. S.; Asher, S. A. *J. Appl. Phys.* **1992**, *71*, 1116.

(19) Tse, A. S.; Wu, Z.; Asher, S. A. *Macromolecules* **1995**, *28*, 6533.

Figure 1. Crystalline colloidal array composed of a BCC array of negatively charged colloidal particles. The colloidal particle charges derive from ionized surface sulfonate groups. The counterions in the surrounding medium maintain the system net neutrality.

Figure 2. Transmission spectrum of a 1.0 mm thick crystalline colloidal array formed from 131-nm diameter poly(heptafluorobutyl methacrylate) particles. The particle volume fraction was 6.13%.

Figure 3. Transmission spectra of 155-nm diameter poly(heptafluorobutyl methacrylate) crystalline colloidal array before and after solidification in a polyacrylamide hydrogel matrix.

Figure 4. Temperature dependence of the PNIPAM colloid diameter and turbidity. The diameter was determined using a commercial quasielastic light scattering apparatus (Malvern Zetasizer 4). The turbidity was measured for a disordered dilute dispersion of these PNIPAM colloids by measuring light transmission through a 1.0 cm pathlength quartz cell with a UV-visible-near IR spectrophotometer. Solids content of the sample in the turbidity experiment was 0.071%, which corresponds to a particle concentration of 2.49×10^{12} spheres/cc. Also shown is the temperature dependence of the turbidity of this random colloidal dispersion. The light scattering increases as the particle becomes more compact due to its increased refractive index mismatch from the aqueous medium (*16*) (Adapted from ref. 16).

Figure 5. Diffraction from a CCA of PNIPAM spheres at 10°C and at 40°C. The spectra were recorded using a UV-visible-near IR spectrophotometer (Perkin Elmer λ-9). The dispersion was contained in a 1.0 mm quartz cuvette oriented at normal incidence to the incident beam. The observed diffraction switching behavior was reversible; these spectra were recorded after the seventh consecutive heat-cool cycle. Inset: Pictorial representation of the temperature switching between a swollen sphere array below the phase transition temperature and an identical compact sphere array above the transition (Adapted from ref. 16).

Figure 6. Temperature tuning of Bragg diffraction from a 125-μm-thick PCCA film of 99-nm polystyrene spheres embedded in a PNIPAM gel. The diffraction wavelength shift results from the temperature-induced volume change of the gel, which alters the lattice spacing. Spectra were recorded in a UV-visible-

near IR spectrophotometer with the sample placed normal to the incident light beam (Adapted from ref.16).

Figure 7. Primary and secondary diffraction from a 6.1-μm thick crystalline colloidal array. A. Primary diffraction at λ_0 from the BCC (110) plane in first order. B. Intense secondary diffraction at $\lambda_0/2$ due to superposition of diffraction from numerous lattice planes.

Figure 8. Schematic of the experimental apparatus for optical nonlinear diffraction measurements.

Figure 9. Transmission spectrum of a 138-nm dyed poly(heptafluorobutyl methacrylate) crystalline colloidal array solidified in a polyacrylamide hydrogel matrix. A: Dye absorption peak. B: CCA diffraction peak.

Figure 10. Pump beam energy dependence of Bragg diffraction intensity. The relative value of Bragg diffraction intensities (R_{on}/R_{off}) were monitored at various pump beam energies. • dyed CCA hydrogel in the medium of water and DMSO at n=1.3908; Δ at n=1.3813; ▪ undyed CCA hydrogel in the medium at n=1.3875.

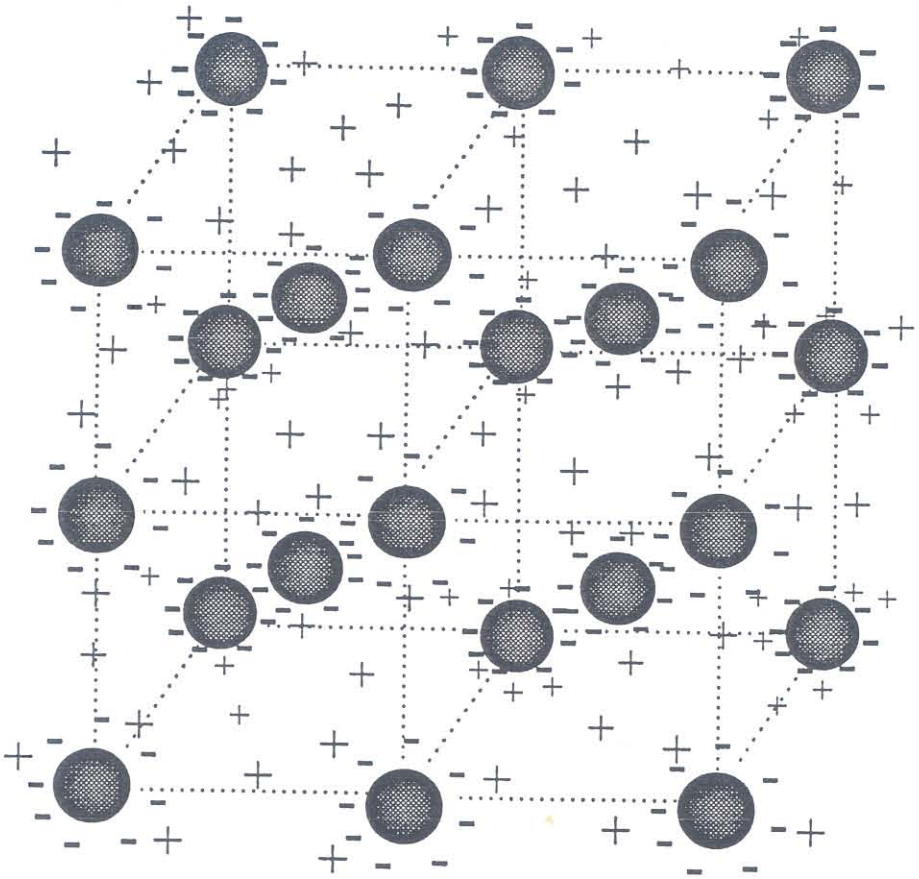

Figure 1. Asher et.al.

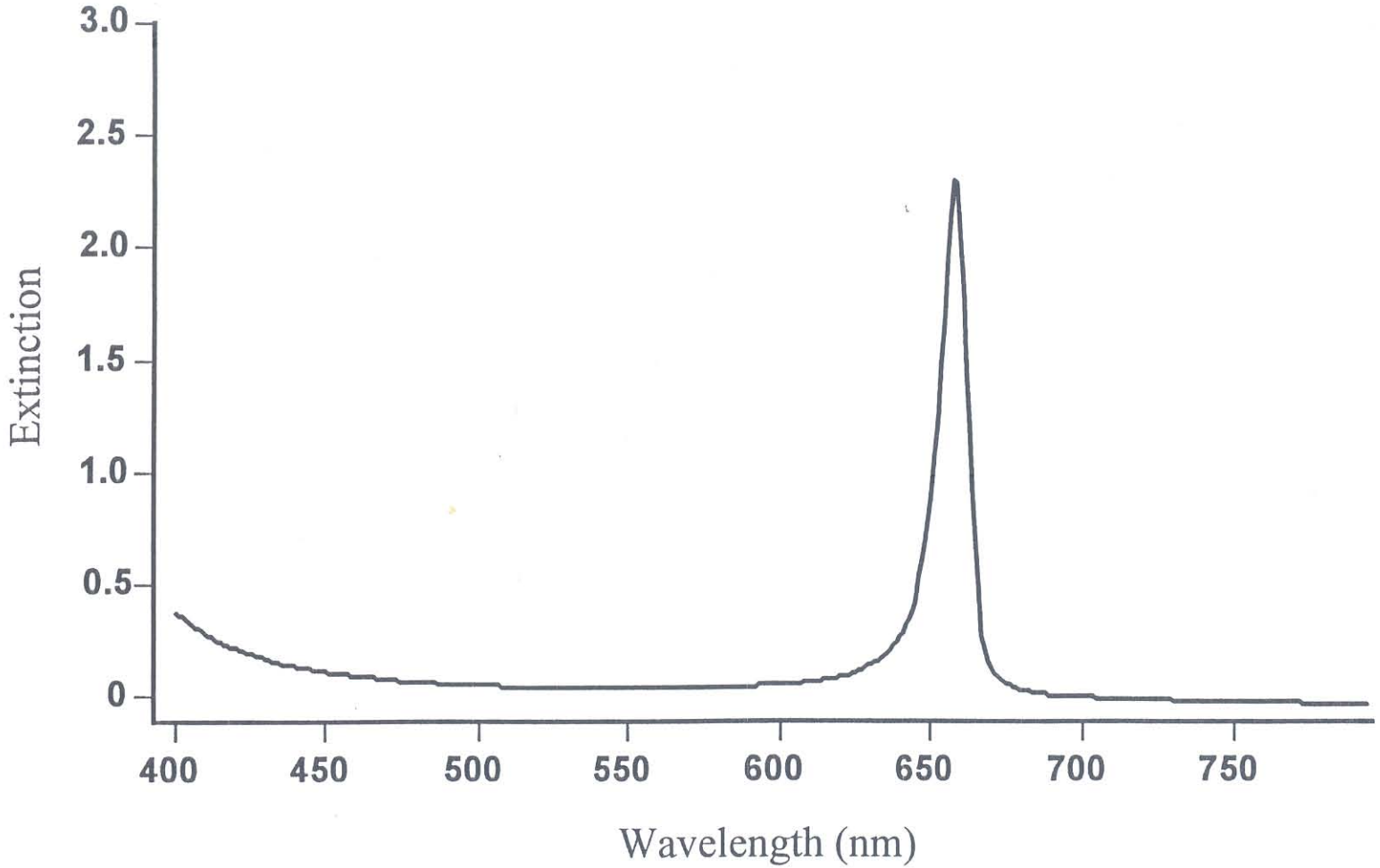

Figure 2. Asher et. al

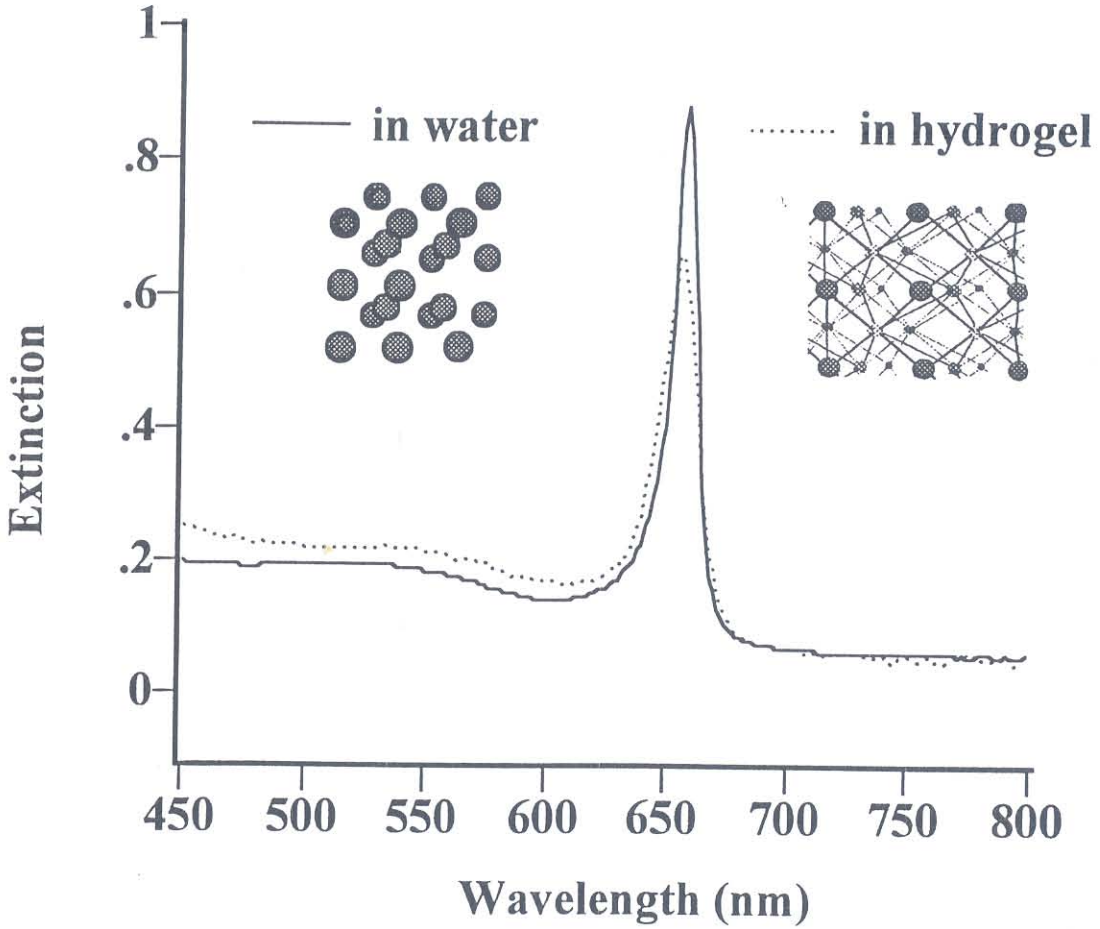

Figure 3. Asher et.al.

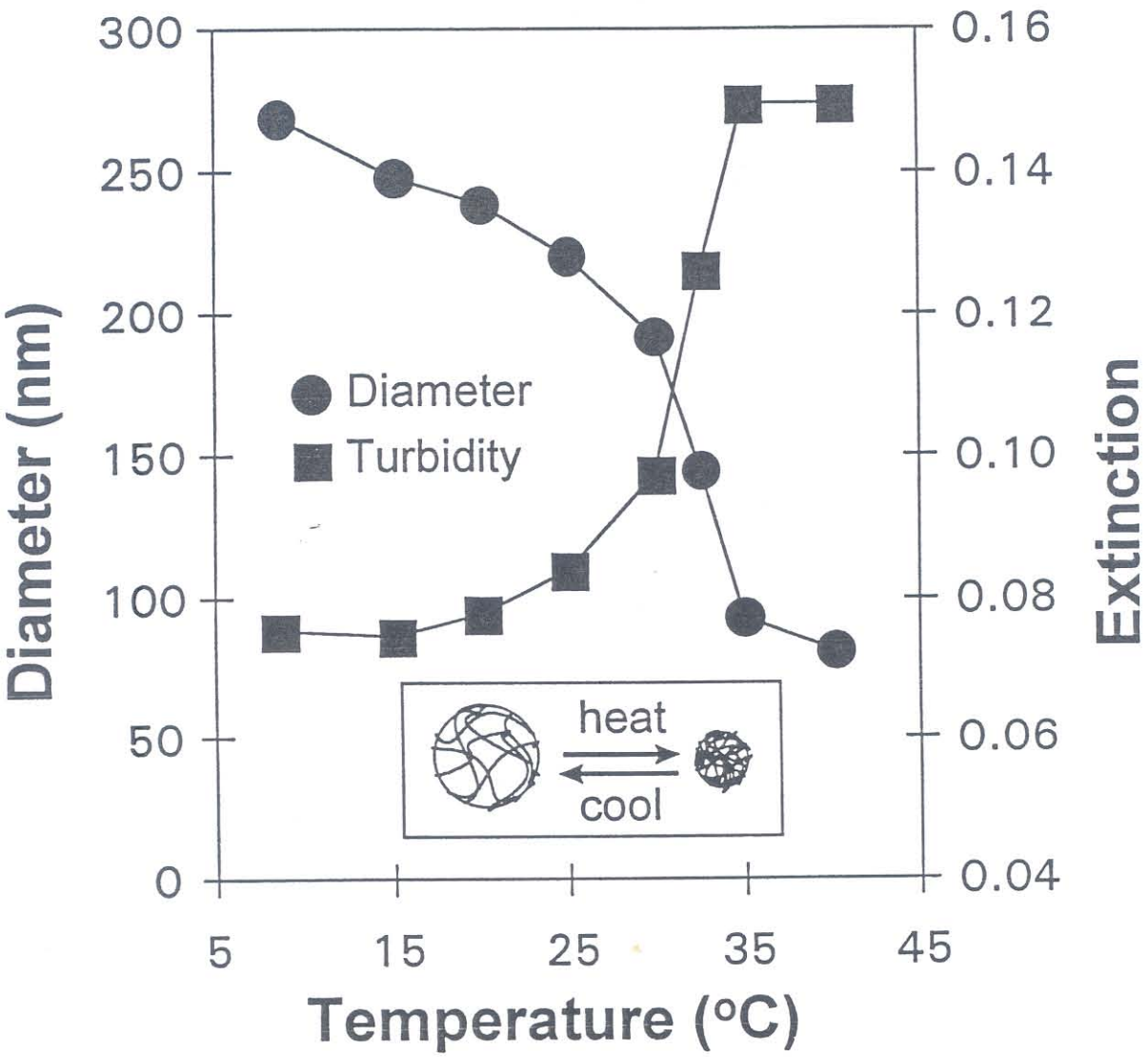

Figure 4. Asher et. al

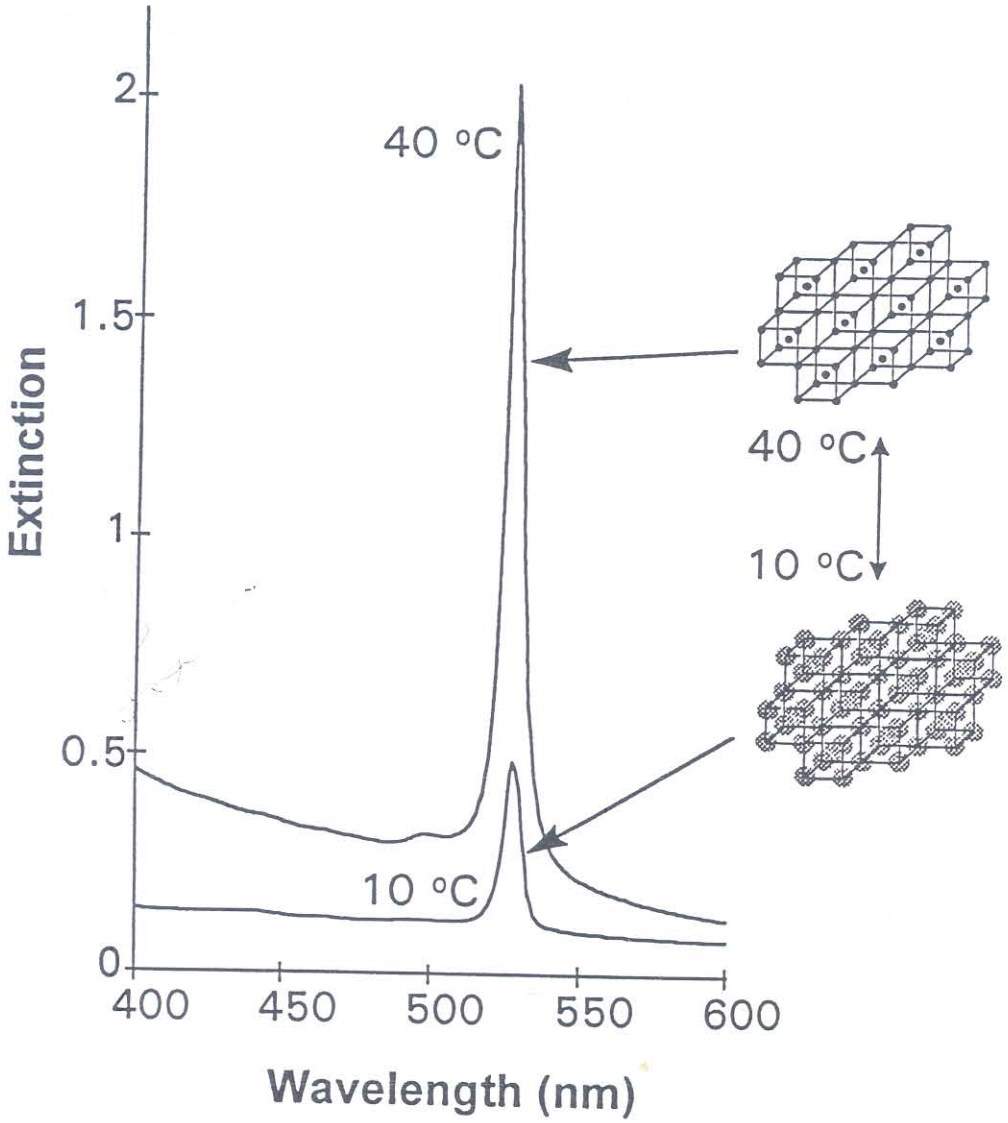

Figure 5. Asher et al

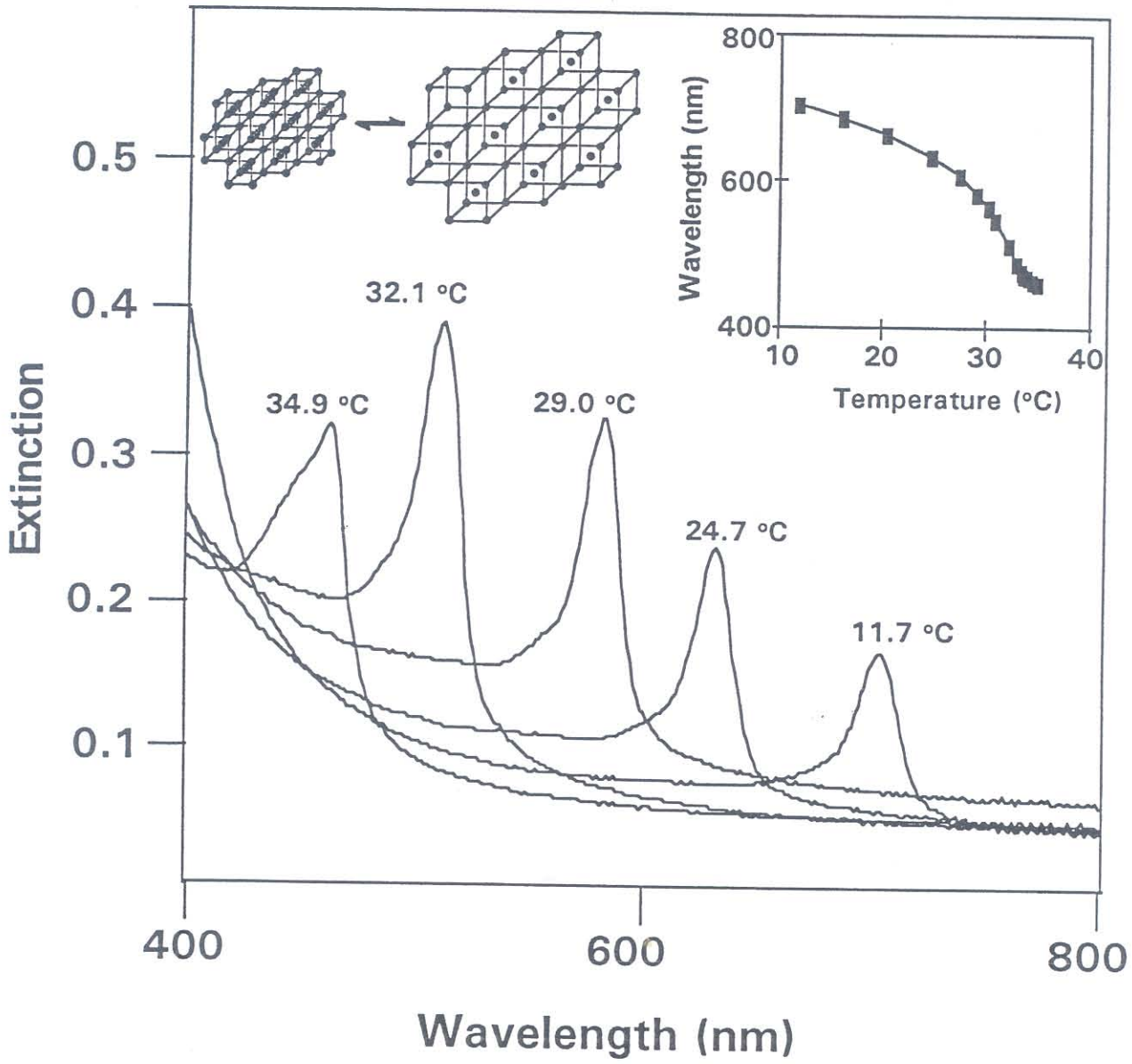

Figure 6. Ashen et. al

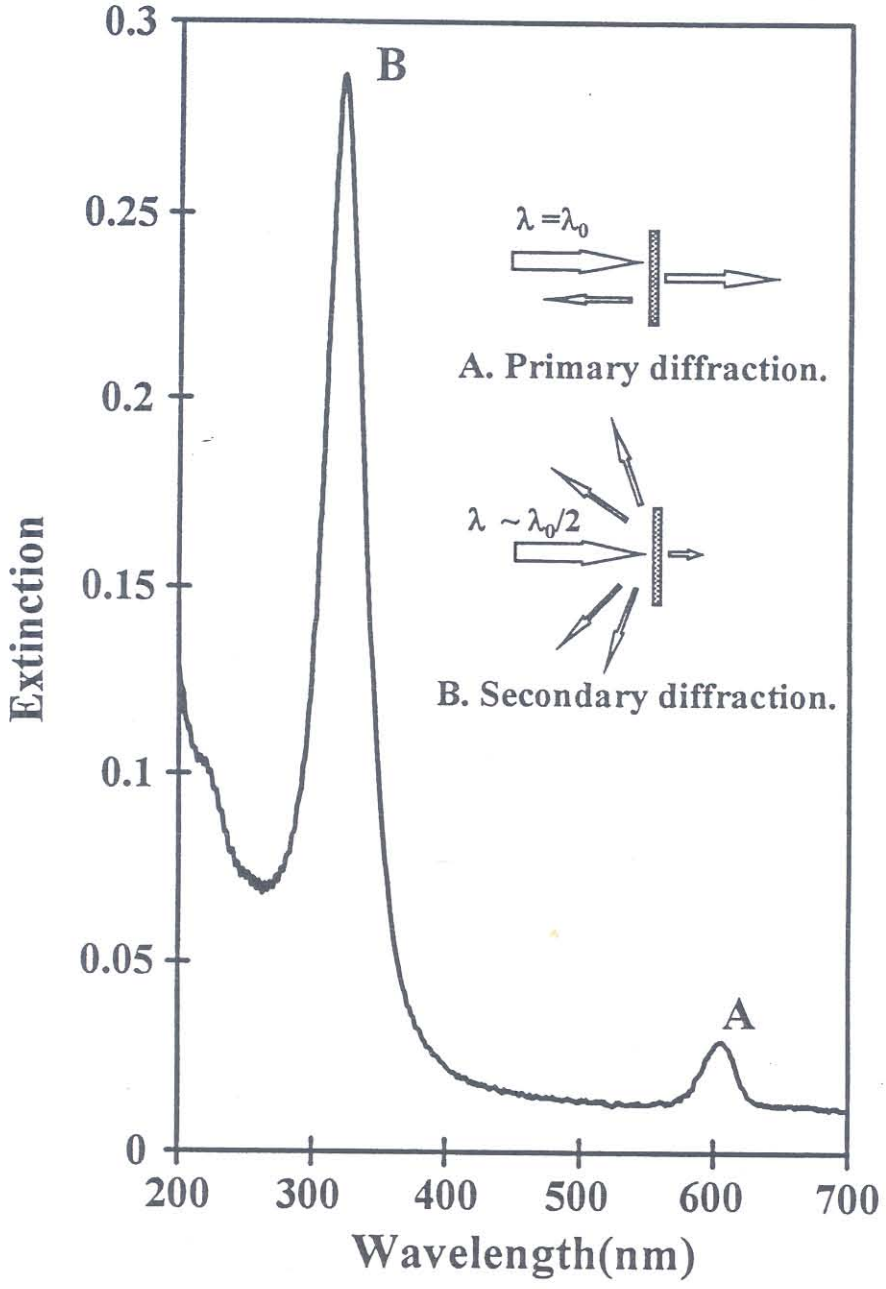

Figure 7. Asher et. al

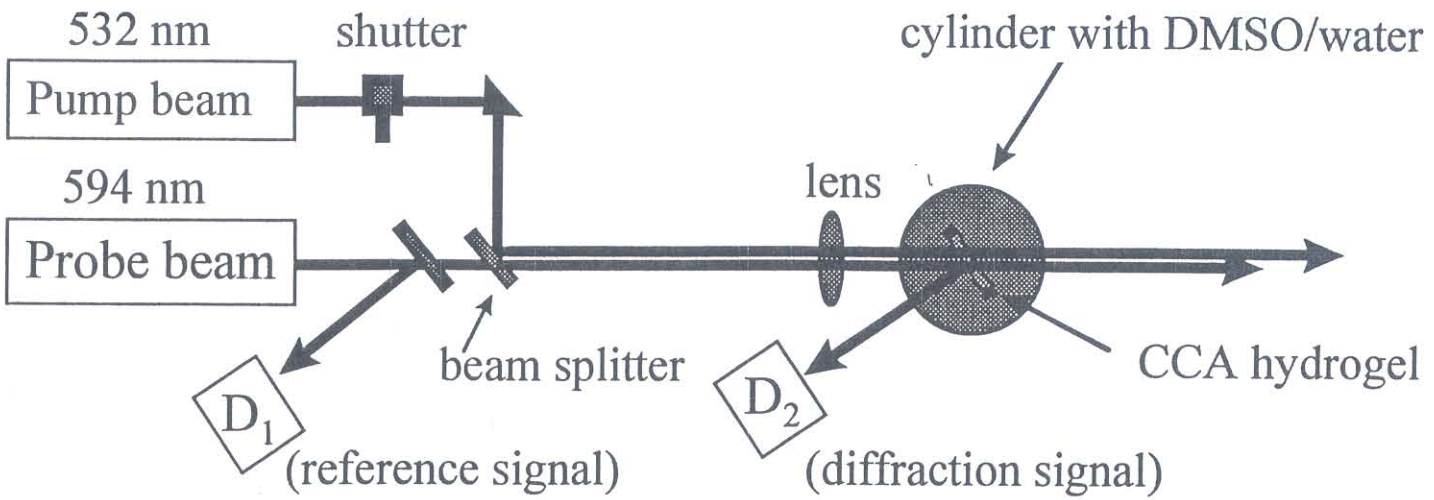

Figure 8. Ashan et. al.

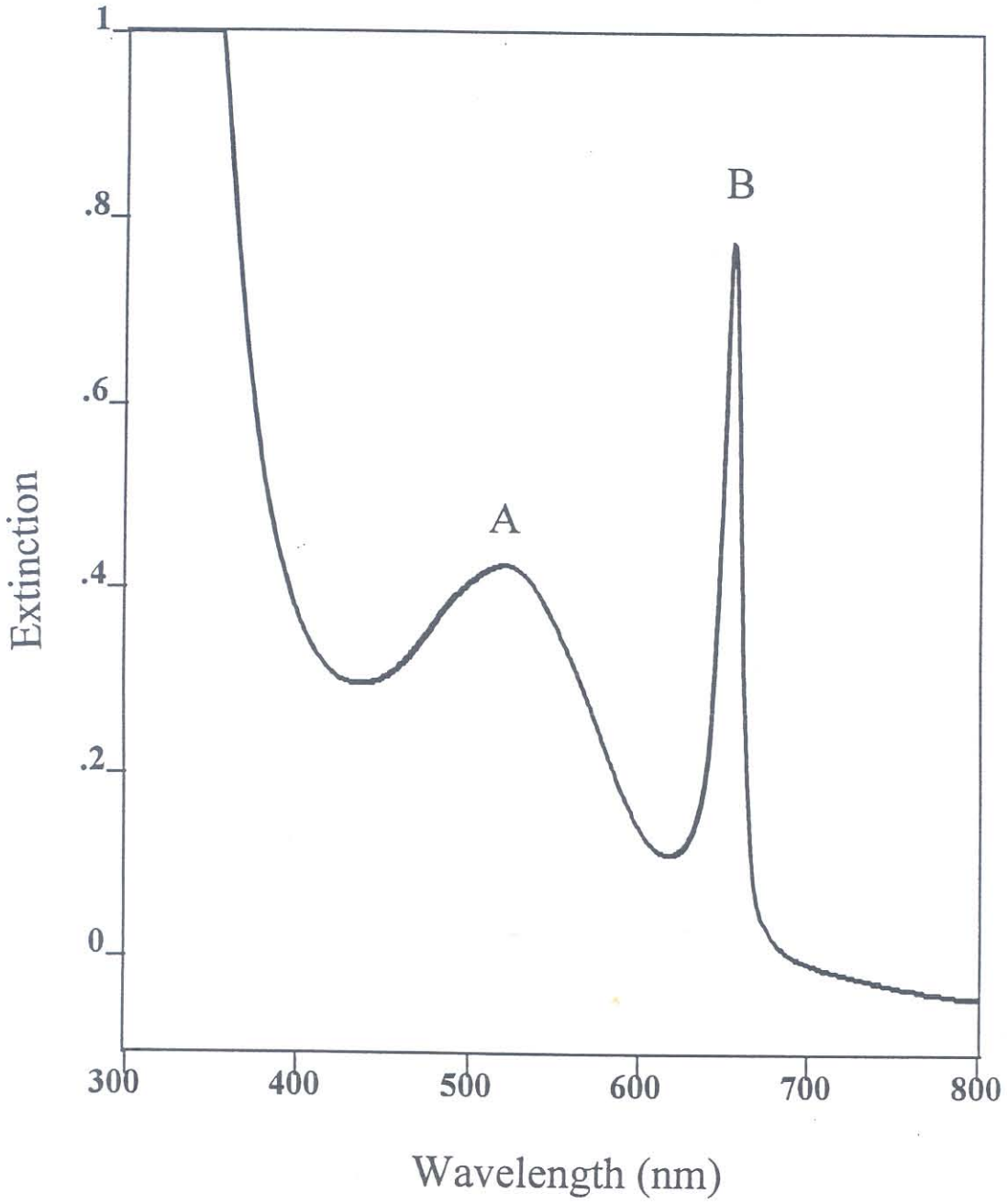

Figure 9. Asher et. al.

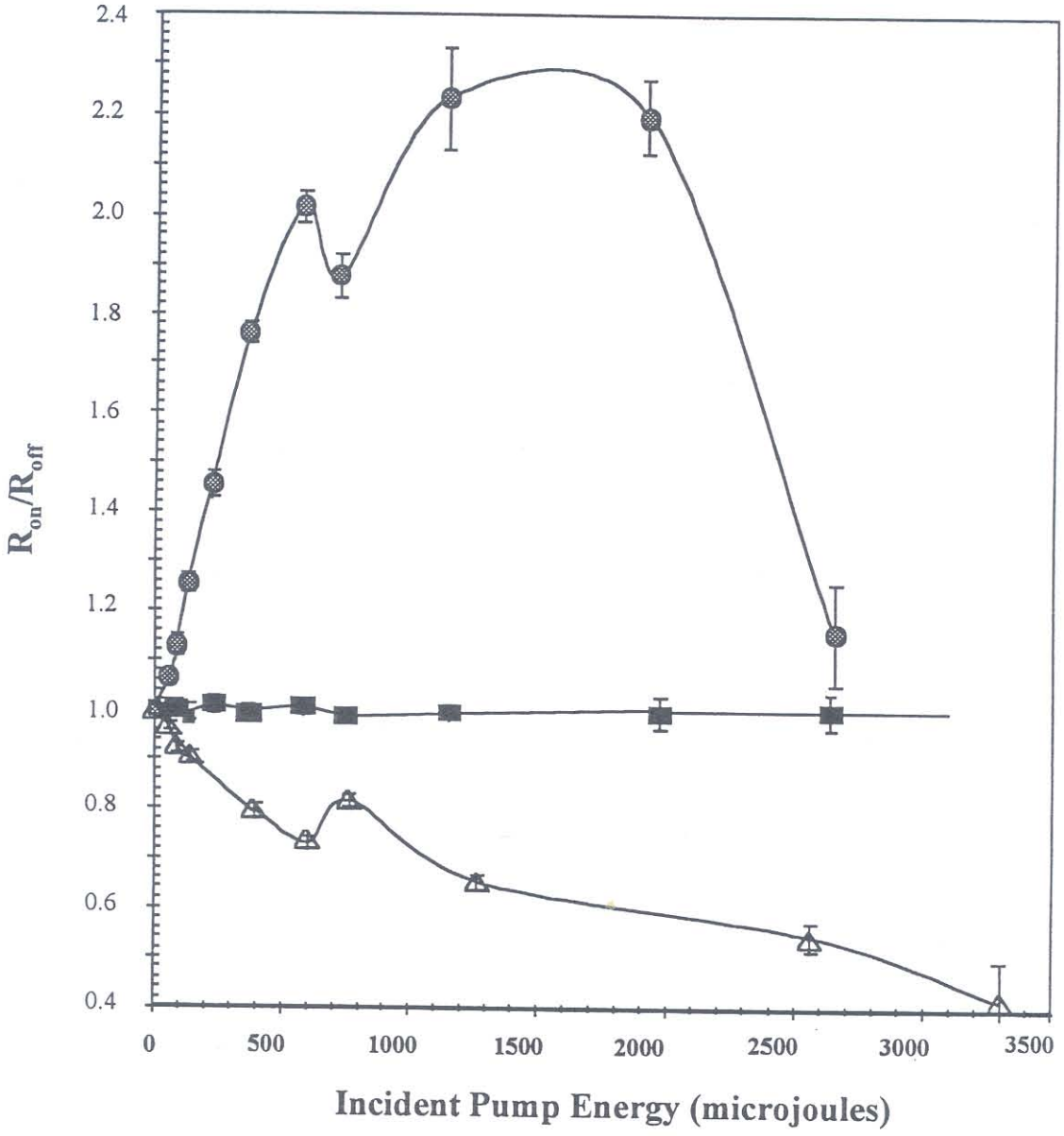

Figure 10. Asher et. al.